

Supporting Information for

Viscosity and liquid-liquid phase separation in healthy and stressed plant SOA

by

*Natalie R. Smith,^a Giuseppe Crescenzo,^b Yuanzhou Huang,^b Anusha P. S. Hettiyadura,^c Kyla
Siemens,^c Ying Li,^a Celia L. Faiola,^{a,d} Alexander Laskin,^c Manabu Shiraiwa,^a Allan K. Bertram,^{*b}
Sergey A. Nizkorodov^{*a}*

(1) Department of Chemistry, University of California, Irvine, Irvine, CA 92697, USA

(2) Department of Chemistry, University of British Columbia, Vancouver, BC

(3) Department of Chemistry, Purdue University, West Lafayette, IN 47907, USA

(4) Department of Ecology and Evolutionary Biology, University of California Irvine, Irvine, CA
92697, USA

**To Whom Correspondence Should be Addressed*

Table S1: Chemical composition of the VOC mixture used to produce SOA; purity and sources of commercially-available standards used to generate healthy and stressed VOC mixtures; and lifetimes with respect to oxidation in the chamber. Monoterpene is abbreviated as MT and sesquiterpene is abbreviated as SQT.

VOC type	Chemical Species	Healthy (mol/mol%)	Stressed (mol/mol %)	Purity	Source	Lifetime (h)
MT	α -phellandrene	20.3%	-	$\geq 75\%$ stabilized ($\leq 0.050\%$ a-tocopherol)	Sigma (CAS:99-83-2)	0.63 ^a
MT	β -pinene	4.6%	-	98%	Acros Organics (CAS: 18172-67-3)	2.66 ^a
MT	α -pinene	2.3%	29.4%	98%	Acros Organics (CAS:7785-26-4)	3.78 ^a
MT	3-carene	53.9%	22.3%	90%	Aldrich (CAS: 13466-78-9)	2.25 ^a
MT	camphene	13.8%	6.3%	$\geq 96\%$	Sigma Aldrich (CAS: 79-92-5)	3.73 ^a
MT	myrcene	-	10.0%	$>75\%$ (Contains 1000 ppm of BHT as inhibitor)	Aldrich (CAS:123-35-3)	0.92 ^a
MT	limonene	-	7.3%	97% Stabilized	Alfa Aesar, (CAS:5989-27-5)	1.21 ^a
SQT	β -caryophyllene	5.2%	3.4%	98.5%	Sigma (CAS:87-44-5)	1.00 ^a
SQT	mix of farnesene isomers ^c	-	12.8%	stabilized ($<0.10\%$ a-tocopherol)	Sigma-Aldrich (Product#: W383902)	1.16 ^b
SQT	valencene	-	8.5%	$\geq 70\%$	Aldrich (CAS:4630-07-3)	N/A

^a Lifetimes calculated using k-values reported in Atkinson et al. (2003).¹ ^b Calculated using k-values for (E)-b-farnesene reported in Kourtchev et al. (2012).² ^c May contain sesquiterpenes, trans- β -farnesene, cis- α -farnesene, trans- α -farnesene, and bisabolene.

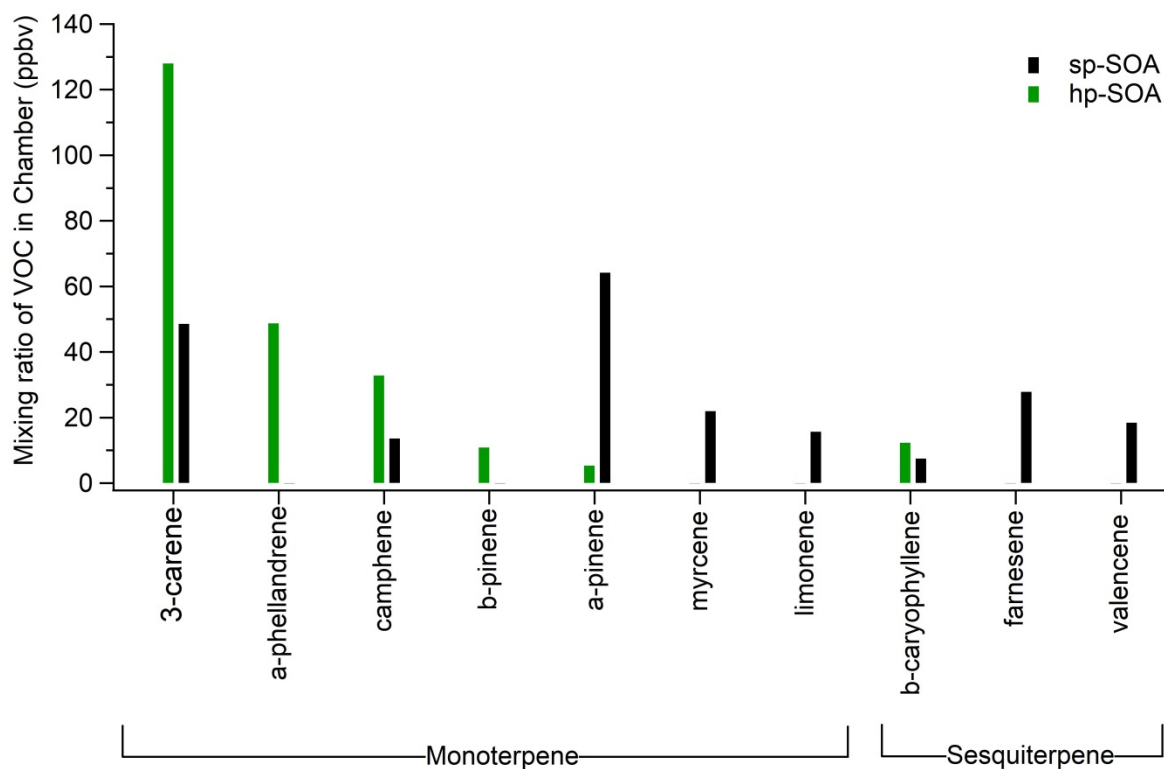


Figure S1. Mixing ratio of each VOC after the injection into the environmental chamber. The relative VOC amounts (Table S1) were chosen to replicate the emission profile of healthy (green) and aphid-stressed (black) Scots Pine trees reported in Faiola et al. (2019).³ We note that the farnesene isomer mixture contained bisabolene and other sesquiterpenes according to Ylisirniö et al. (2020),⁴ but they are all lumped into the farnesene bar.

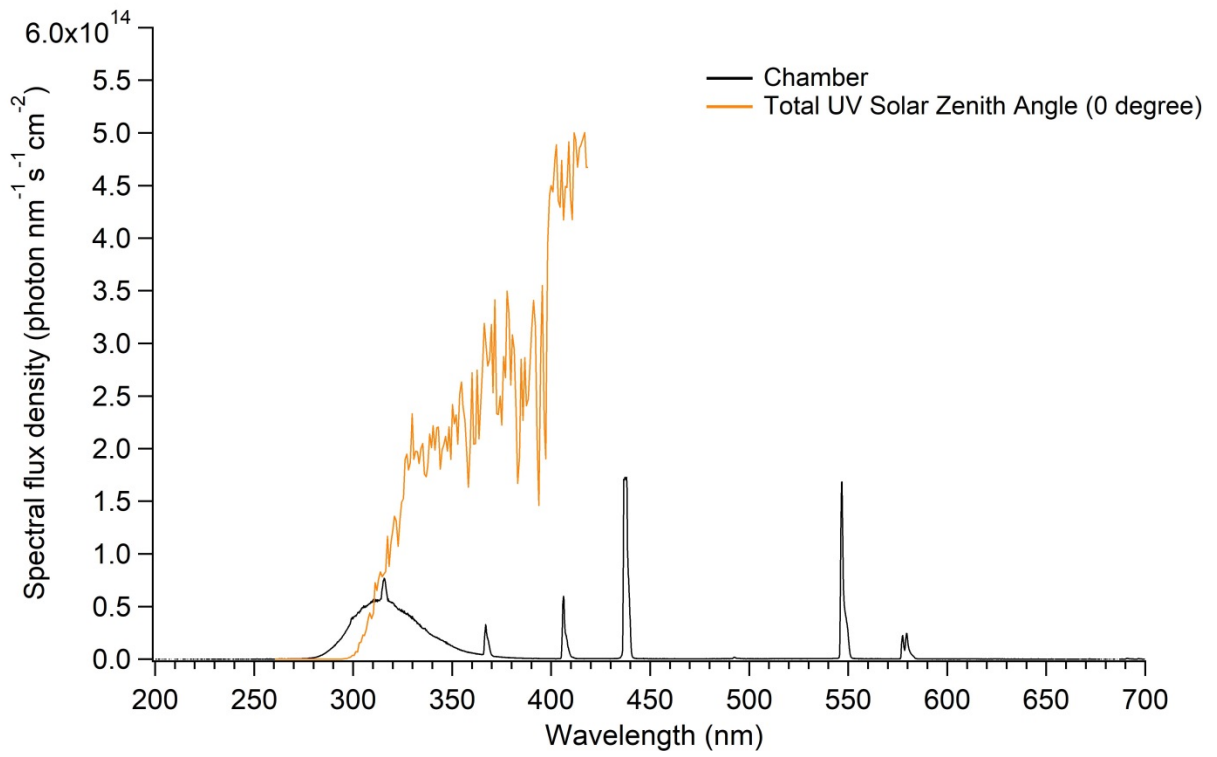


Figure S2: Measured spectral flux density in chamber compared to the solar spectral flux density calculated at a solar zenith angle of 0 degrees.

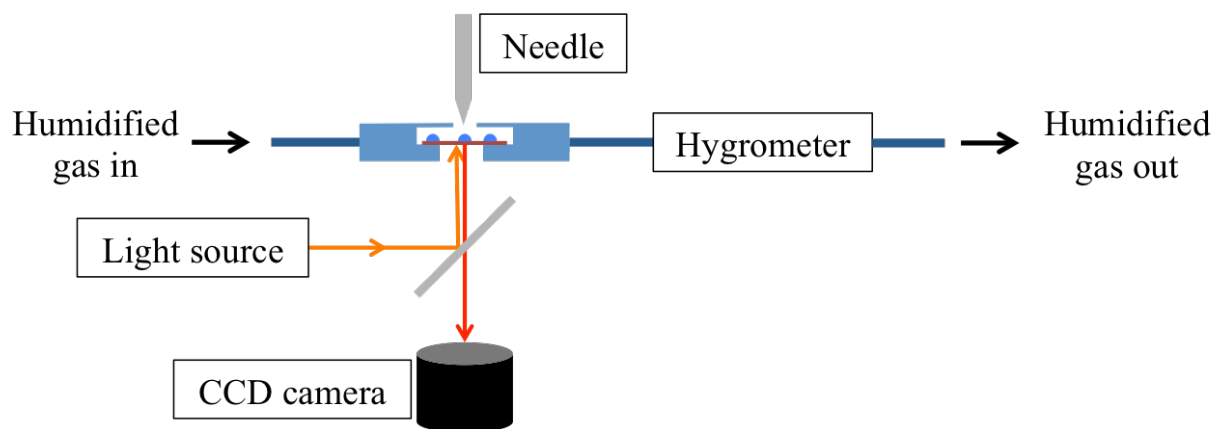


Figure S3: Schematic representation of the poke-flow experimental apparatus.

Table S2: COMSOL parameters used for simulating the upper and lower limits of viscosity of the collected SOA by poke-flow.

SOA type		Surface tension (mN m ⁻¹)	Slip length (m)	Contact angle (°)
Heathy plant SOA	Range of values	25.3 ^a -45 ^b	5x10 ⁻⁹ -1x10 ⁻⁶ ^c	50.9-60.0 ^d
Stressed plant SOA	Range of values	23.0 ^e -45 ^b	5x10 ⁻⁹ -1x10 ⁻⁶ ^c	54.2-63.8 ^d
α-pinene SOA	Range of values	25.3 ^z -45 ^b	5x10 ⁻⁹ -1x10 ⁻⁶ ^c	52.7-67.7

^a As a conservative lower limit to the surface tension of the healthy plant SOA, we used the surface tension of liquid 3-carene. ^b 3-Carene has the lowest surface tension of all the VOCs used to model healthy plant emissions. Surface tension of liquid α-pinene. Surface tensions were determined with the ACD/Labs Percepta Platform-PhysChem Module, retrieved from Chemspider July 12, 2019. ^b This upper limit is consistent with surface tension measurements of SOA at RH ≲65% RH and surface tensions reported for alcohols, organic acids, esters, and ketones, as well as surface tension measurements of water solutions containing SOA products. ^c Range based on measurements of the slip length of organic compounds and water on hydrophobic surfaces.⁵⁻¹⁷ ^d The contact angle was determined by measuring the height and radii of individual droplets using a confocal microscope. Note: the simulated viscosities depend only weakly on the contact angle. Changing the contact angle by ±10% changes the simulated viscosity on average by ±15%, which is small compared to the overall uncertainties associated with the simulated viscosities. ^e As a conservative lower limit to the surface tension of the stressed plant SOA, we used the surface tension of liquid myrcene. Myrcene has the lowest surface tension of all the VOCs used to model stressed plant emissions. Surface tensions were determined with the ACD/Labs Percepta Platform-PhysChem Module, retrieved from Chemspider July 12, 2019.

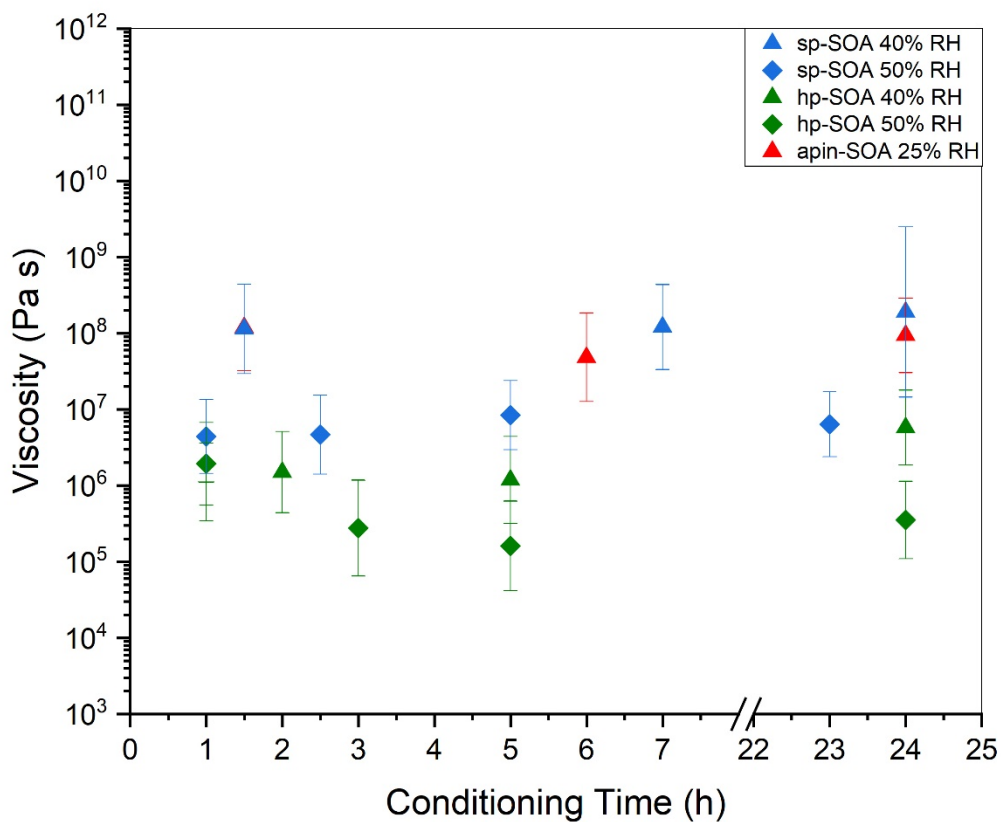


Figure S4: Particle viscosity as a function of conditioning time in poke-flow cell at humidity of interest. Vertical bars represent the calculated lower and upper limits of viscosity (83% confidence interval) based on COMSOL simulations (see Table S2 for input parameters).

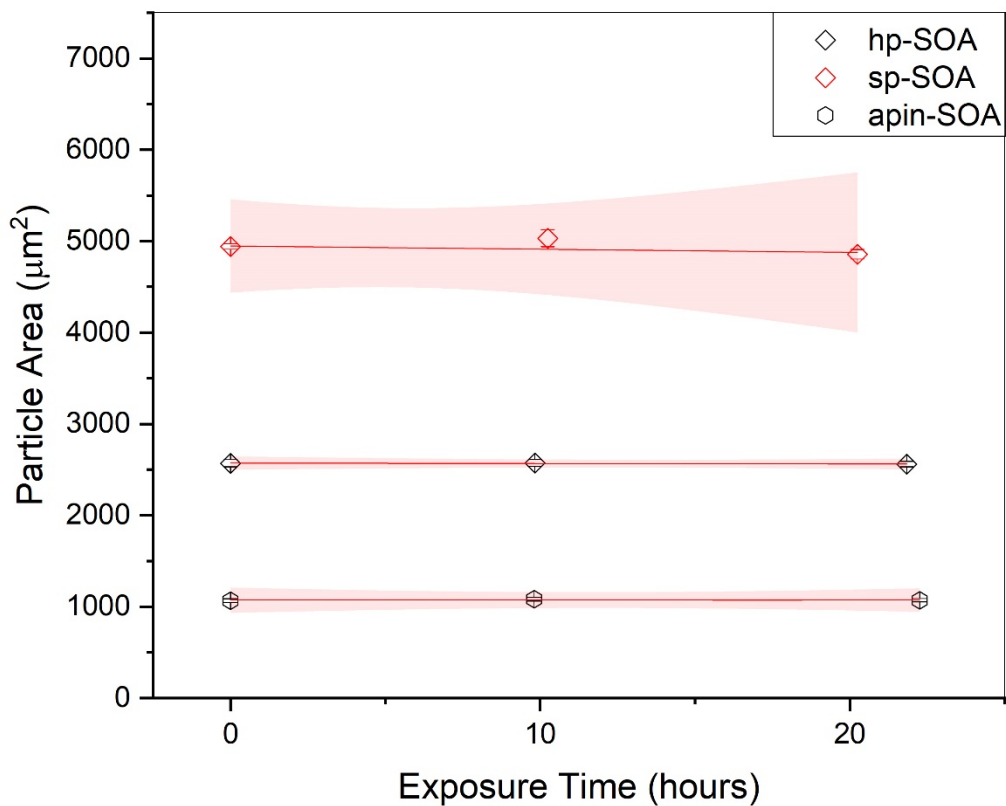


Figure S5: Particle area as a function of exposure time to dry (< 0.5% RH) nitrogen gas flow, shaded red regions indicates the 95% confidence bands. The lack of change suggests that particles are stable with respect to evaporation over the experimental time scale.

Calculations for mixing time of water within SOA

Mixing times of water within SOA were determined for a 50 μm macroparticle at 293 K, which corresponds to the approximate size of collected macroparticles and temperature at which experiments were performed for the hp-SOA and sp-SOA in this study. The fractional Stokes-Einstein equation was used to determine diffusion coefficients for water as a function of RH and temperature:¹⁸⁻²⁰

$$D_{H_2O}(RH, T) = D_0(T) \times \left(\frac{\eta_0(T)}{\eta(RH, T)} \right)^\xi$$

where $D_{H_2O}(RH, T)$ is the RH and temperature dependent diffusion coefficient of water in SOA, $D_0(T)$ is the temperature dependent diffusion coefficient of water in pure water (calculated using Equation. (1) in the main text), ξ is the fractional exponent, $\eta_0(T)$ is the temperature-dependent viscosity of pure water at 293 K, and $\eta(RH, T)$ is the calculated viscosity of the hp-SOA or sp-SOA at a specific RH and 293 K. The temperature-dependent viscosity data for pure water were taken from Hallett (1963) and Crittenden et al. (2012).^{21,22} $D_0(T)$ was evaluated using the Stokes-Einstein equation and assuming a radius for pure water of 0.1 nm.²⁰ The value of the fractional exponent was calculated using the equation below:¹⁸

$$\xi = 1 - \left[A \times \exp \left(-B \frac{R_{diff}}{R_{matrix}} \right) \right]$$

where A and B are coefficients with values of 0.73 ± 0.12 and 1.79 ± 0.29 , respectively. To evaluate the fractional exponent, we assumed $R_{diff} = 0.1$ nm and $R_{matrix} = 0.4$ nm to be consistent with the size of organic molecules discussed above. The fractional Stokes-Einstein equation is able to predict 98 % of the published diffusion coefficients of small molecules, including water, within the uncertainties of the measurements for organic-water mixtures.¹⁸ Once $D_{H_2O}(RH, T)$ was determined using the equations above, we then calculated mixing times of water within the SOA using an equation similar to Equation (2) in the main text. The results of this calculation are shown in Figure S6.

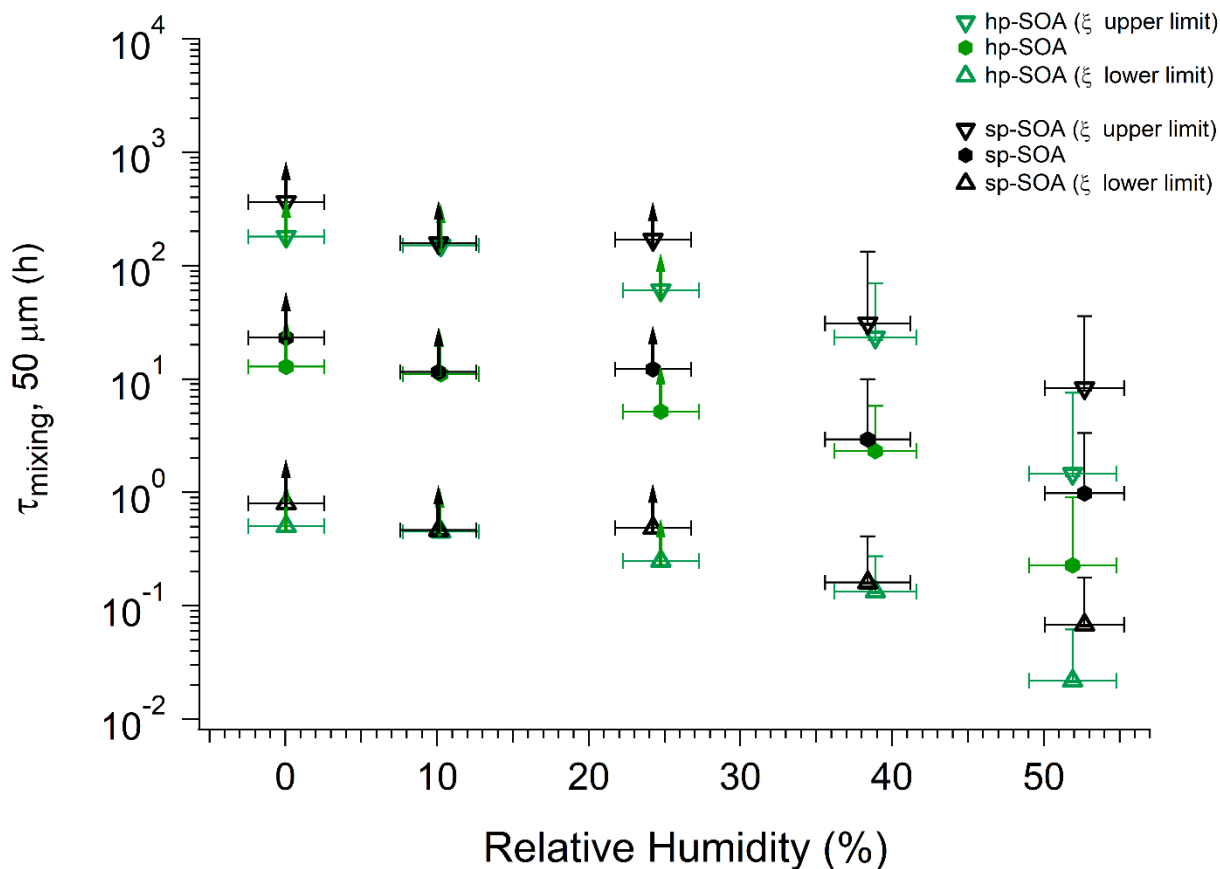
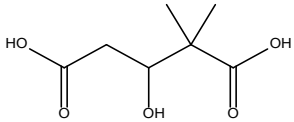
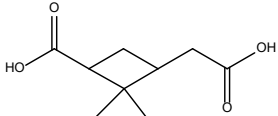
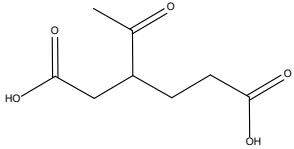
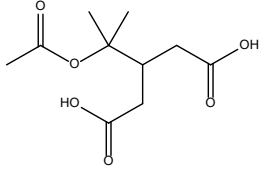
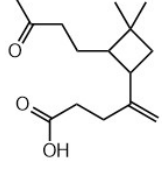
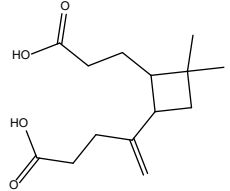
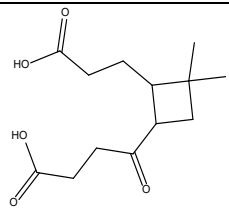
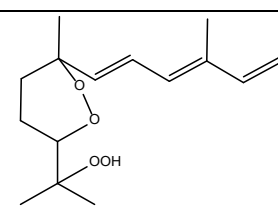


Figure S6: Mixing times of water within a $50 \mu\text{m}$ sized macroparticle ($\tau_{\text{mixing}, 50 \mu\text{m}}$) for hp-SOA (green hexagons) and sp-SOA (black hexagons). Error in the RH measurement was $\pm 2.5\%$. Upward arrows indicate lower limits. Vertical bars represent the calculated lower and upper limits of $\tau_{\text{mixing}, 50 \mu\text{m}}$ (83% confidence interval) based on COMSOL simulations (see Table S2 for input parameters). $\tau_{\text{mixing}, 50 \mu\text{m}}$ was also calculated using upper ($A= 0.61$, $B= 2.08$) and lower limits ($A=0.85$, $B=1.50$) for uncertainty in the fractional exponent (ξ).

Table S3: The most abundant formulas detected by nano-DESI-HRMS. All of these compounds appear in both (+) and (-) ESI modes; the second column lists the ionization mode in which they have higher relative peak abundance. References for previously reported structures identified as a monoterpene oxidation product (MTOX) or sesquiterpene oxidation product (SQTOX) that have the same neutral molecular formula and mass as those found in this study are listed in the last column.

Neutral Mass (Da)	Prominent Ionization Mode (-/+) and sample	Neutral molecular Formula	Name	Previously Reported Structures ^a	References
176.07	(-) hp-SOA	C ₇ H ₁₂ O ₅	3-hydroxy-2,2-dimethyl glutaric acid		MTOX (Haddad et al 2011) ²³
186.09	(-) sp-SOA	C ₉ H ₁₄ O ₄	Pinic acid limononic acid		MTOX (Yee et al 2018) ²⁴ (Jaoui et al 2006) ²⁵ (Fang et al 2017) ²⁶
188.07	(-) hp-SOA	C ₈ H ₁₂ O ₅	Ketolimonic acid		MTOX (Jaoui et al 2006) ²⁵
232.09	(-) hp-SOA	C ₁₀ H ₁₆ O ₆	Diaterpenylic acid acetate		MTOX (Yee et al 2018) ²⁴
252.17	(-) sp-SOA	C ₁₅ H ₂₄ O ₃	β-caryophyllonic acid		SQTOX (Yee et al 2018) ²⁴
254.15	(-) sp-SOA (+) hp-SOA	C ₁₄ H ₂₂ O ₄	β-caryophyllinic acid		SQTOX (Yee et al 2018) ²⁴

256.13	(+/-) hp-SOA	C ₁₃ H ₂₀ O ₅	β-nocaryophyllinic acid		SQTOX (Yee et al 2018) ²⁴
268.17	(+/-) sp-SOA (+) hp-SOA	C ₁₅ H ₂₄ O ₄	----- (Conjugated triene hydroperoxide)		SQTOX (Jaoui et al 2016) ²⁷
302.17	(+) sp-SOA	C ₁₅ H ₂₆ O ₆	-----		
318.17	(+) sp-SOA	C ₁₅ H ₂₆ O ₇	-----		

^a Tentatively assigned structures as MS/MS has not been performed.

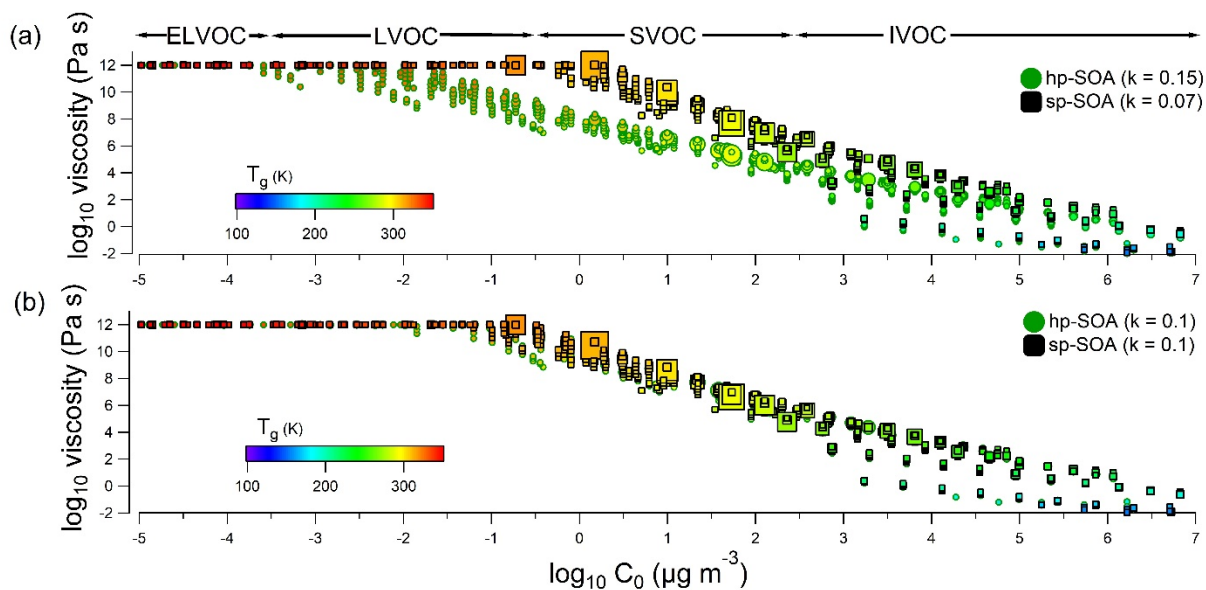


Figure S7: (a) viscosity of individual SOA compounds at 50% RH and 291 K as a function of C_0 in healthy ($\kappa = 0.15$) and stressed ($\kappa = 0.07$) plant SOA. (b) Viscosity of individual SOA compounds at 50% RH and 291 K as a function of C_0 with $\kappa = 0.1$ applied to both healthy and stressed plant SOA. In each panel, the warmer the color, the higher the glass transition temperature. The larger the circle or square marker size, the larger the relative abundance of the species based on the HRMS analysis.

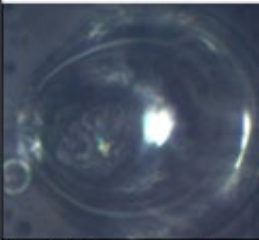
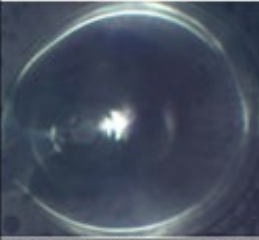
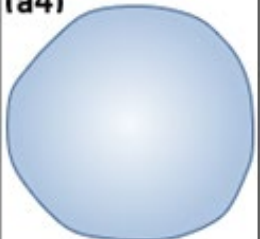
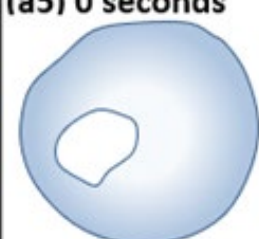
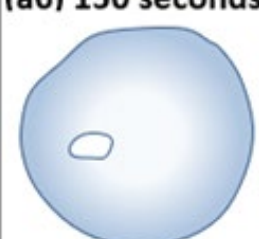
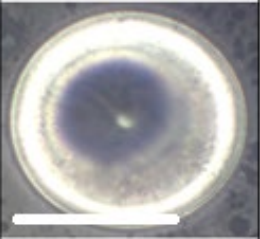
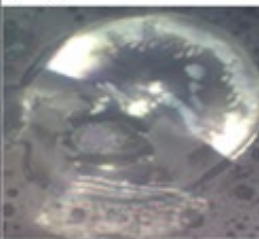
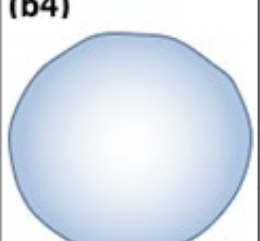
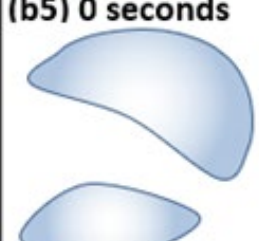
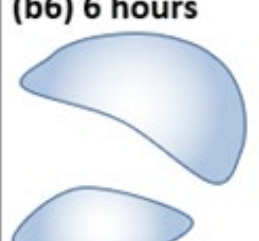
Relative humidity	Pre-poking	Poking	First frame post-poking	Post-Poking
(a) 50%	(a1) 		(a2) 0 seconds 	(a3) 150 seconds 
	(a4) 		(a5) 0 seconds 	(a6) 150 seconds 
(b) 0%	(b1) 		(b2) 0 seconds 	(b3) 6 hours 
	(b4) 		(b5) 0 seconds 	(b6) 6 hours 

Figure S8: Optical images of SOA particles produced from photooxidation of VOCs from healthy trees during a poke-flow experiment at a) 50%, and b) 0% RH. Images a1) and b1) are pre-poking images. a4) and b4) are demonstrative diagrams of pre-poking. a2) and b2) are the first frame post-poking. a5) and b5) are demonstrative diagrams of the first frame post-poking. a3) and b3) are the post-poking images at 150 s and 6 hrs. a6) and b6) are demonstrative diagrams of post-poking at 150 s and 6 h. The white scale bars correspond to 50 μm .

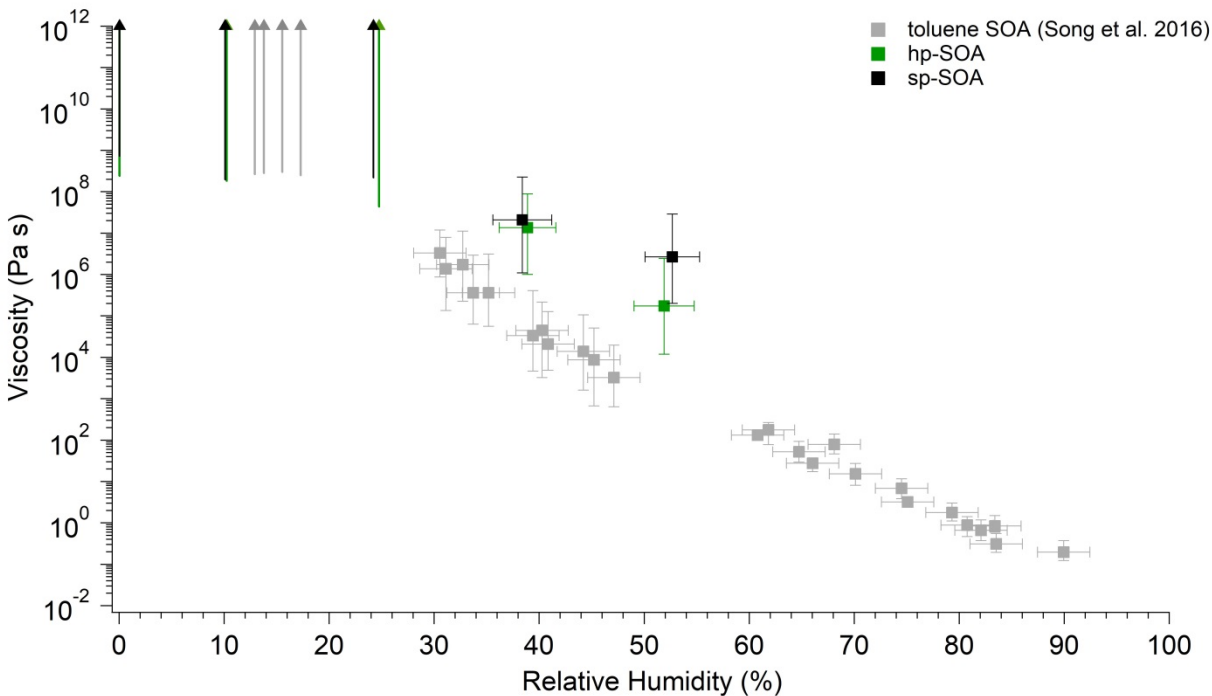


Figure S9: Experimentally determined viscosity of toluene photooxidation SOA reproduced from Song et al. (2016)²⁸ compared to healthy and stressed photooxidation SOA over various relative humidities determined by the poke-flow method. Vertical bars represent the calculated lower and upper limits of viscosity using the COMSOL simulations (see Table S2 for input parameters). Horizontal bars represent the uncertainty in the relative humidity measurement. The upward arrows indicate lower limits of viscosity.

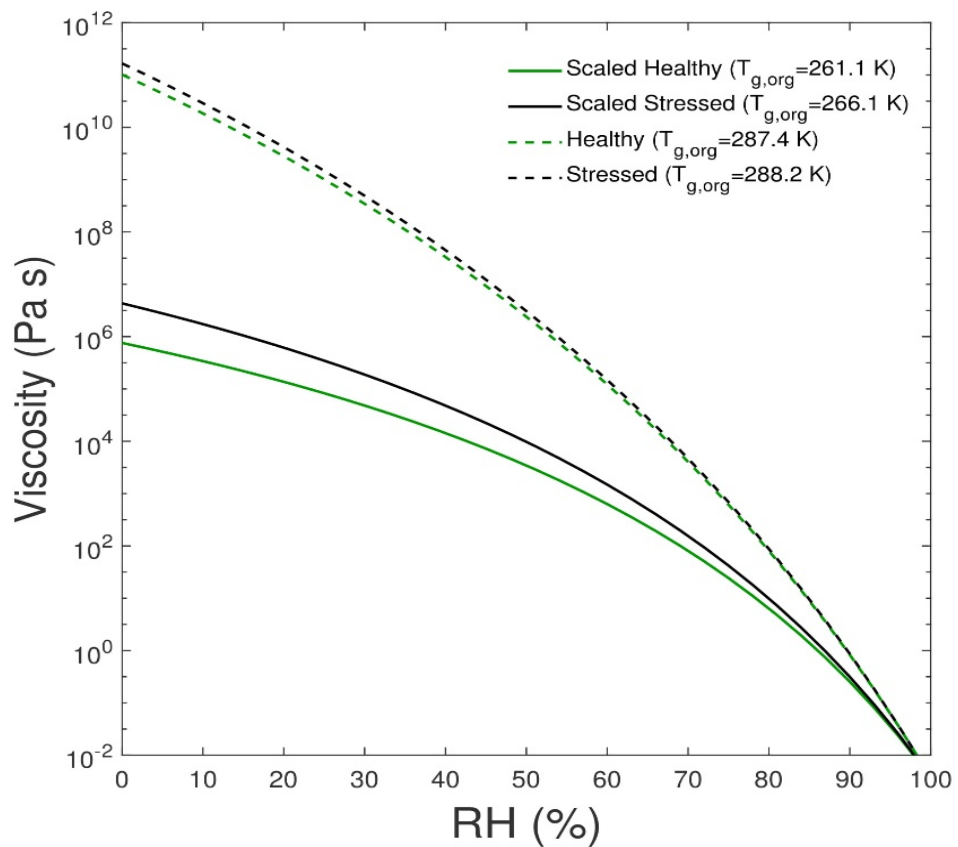


Figure S10: Predicted viscosity as a function of RH using $\kappa = 0.1$ calculated for both healthy and stressed plant SOA using either scaled (solid lines) or unscaled (dashed lines) peak abundances in the mass spectra that combined both positive and negative ion mode peaks.

References

- 1 R. Atkinson and J. Arey, *Chem. Rev.*, 2003, **103**, 4605–4638.
- 2 I. Kourtchev, I. Bejan, J. R. Sodeau and J. C. Wenger, *Atmos. Environ.*, 2012, **46**, 338–345.
- 3 C. L. Faiola, I. Pullinen, A. Buchholz, F. Khalaj, A. Ylisirniö, E. Kari, P. Miettinen, J. K. Holopainen, M. Kivimäenpää, S. Schobesberger, T. Yli-Juuti and A. Virtanen, *ACS Earth Sp. Chem.*, 2019, **3**, 1756–1772.
- 4 A. Ylisirniö, A. Buchholz, C. Mohr, Z. Li, L. Barreira, A. Lambe, C. Faiola, E. Kari, T. Yli-Juuti, S. A. Nizkorodov, D. R. Worsnop, A. Virtanen and S. Schobesberger, *Atmos. Chem. Phys.*, 2020, **20**, 5629–5644.
- 5 J. Baudry, E. Charlaix, A. Tonck and D. Mazuyer, *Langmuir*, 2001, **17**, 5232–5236.
- 6 B. Bhushan, Y. Wang and A. Maali, *Langmuir*, 2009, **25**, 8117–8121.
- 7 D. C. Tretheway and C. D. Meinhardt, *Phys. Fluids*, 2002, **14**, L9–L12.
- 8 O. I. Vinogradova, K. Koynov, A. Best and F. Feuillebois, *Phys. Rev. Lett.*, 2009, **102**, 118302.
- 9 L. Zhu, P. Attard and C. Neto, *Langmuir*, 2012, **28**, 7768–7774.
- 10 J. H. J. Cho, B. M. Law and F. Rieutord, *Phys. Rev. Lett.*, 2004, **92**, 166102.
- 11 N. V Churaev, V. D. Sobolev and A. N. Somov, *J. Colloid Interface Sci.*, 1984, **97**, 574–581.
- 12 C. Cottin-Bizonne, S. Jurine, J. Baudry, J. Crassous, F. Restagno and É. Charlaix, *Eur. Phys. J. E*, 2002, **9**, 47–53.
- 13 C. Cottin-Bizonne, B. Cross, A. Steinberger and E. Charlaix, *Phys. Rev. Lett.*, 2005, **94**, 1–4.
- 14 V. S. J. Craig, C. Neto and D. R. M. Williams, *Phys. Rev. Lett.*, 2001, **87**, 05450414.
- 15 D. Jing and B. Bhushan, *Langmuir*, 2013, **29**, 14691–14700.
- 16 P. Joseph and P. Tabeling, *Phys. Rev. E - Stat. Nonlinear, Soft Matter Phys.*, 2005, **71**, 1–4.
- 17 S. P. McBride and B. M. Law, *Phys. Rev. E*, 2009, **80**, 060601.
- 18 E. Evoy, S. Kamal, G. N. Patey, S. T. Martin and A. K. Bertram, *J. Phys. Chem. A*, 2020, **124**, 2301–2308.
- 19 E. Evoy, A. M. Maclean, G. Rovelli, Y. Li, A. P. Tsimpidi, V. A. Karydis, S. Kamal, J. Lelieveld, M. Shiraiwa, J. P. Reid and A. K. Bertram, *Atmos. Chem. Phys.*, 2019, **19**, 10073–10085.
- 20 H. C. Price, J. Mattsson and B. J. Murray, *Phys. Chem. Chem. Phys.*, 2016, **18**, 19207–19216.
- 21 J. Hallett, *Proc. Phys. Soc.*, 1963, **82**, 1046–1050.
- 22 J. C. Crittenden, R. R. Trussel, D. W. Hand, K. J. Howe and G. Tchobanoglous, *MWH's*

Water Treatment, John Wiley and Sons, 2012.

- 23 I. El Haddad, N. Marchand, B. Temime-Roussel, H. Wortham, C. Piot, J.-L. Besombes, C. Baduel, D. Voisin, A. Armengaud and J.-L. Jaffrezo, *Atmos. Chem. Phys.*, 2011, **11**, 2059–2079.
- 24 L. D. Yee, G. Isaacman-Vanwertz, R. A. Wernis, M. Meng, V. Rivera, N. M. Kreisberg, S. V Hering, M. S. Bering, M. Glasius, M. A. Upshur, A. G. Bé, R. J. Thomson, F. M. Geiger, J. H. Offenberg, M. Lewandowski, I. Kourtchev, M. Kalberer, S. De Sá, S. T. Martin, M. L. Alexander, B. B. Palm, W. Hu, P. Campuzano-Jost, D. A. Day, J. L. Jimenez, Y. Liu, K. A. Mckinney, P. Artaxo, J. Viegas, A. Manzi, M. B. Oliveira, R. De Souza, L. A. T. Machado, K. Longo and A. H. Goldstein, *Atmos. Chem. Phys.*, 2018, **18**, 10433–10457.
- 25 M. Jaoui, E. Corse, T. E. Kleindienst, J. H. Offenberg, M. Lewandowski and E. O. Edney, *Environ. Sci. Technol.*, 2006, **40**, 3819–3828.
- 26 W. Fang, L. Gong and L. Sheng, *Environ. Chem.*, 2017, **14**, 75–90.
- 27 M. Jaoui, M. Lewandowski, K. S. Docherty, E. W. Corse, W. A. Lonneman, J. H. Offenberg and T. E. Kleindienst, *Atmos. Environ.*, 2016, **130**, 190–201.
- 28 M. Song, P. F. Liu, S. J. Hanna, R. A. Zaveri, K. Potter, Y. You, S. T. Martin and A. K. Bertram, *Atmos. Chem. Phys.*, 2016, **16**, 8817–8830.